Journal of Catalysis **200,** 309–320 (2001)
doi:10.1006/jcat.2001.3188, available online at http://www.idealibrary.com on IDEAL®

Palladium–Silver Sol–Gel Catalysts for Selective Hydrodechlorination of 1,2-Dichloroethane into Ethylene

III. Kinetics and Reaction Mechanism

Benoît Heinrichs,*,[1] Jean-Paul Schoebrechts,† and Jean-Paul Pirard*

**Laboratoire de Génie Chimique, B6a, Université de Liège, B-4000 Liège, Belgium; and †Laboratoire Central, Solvay, S.A., Rue de Ransbeek, 310, B-1120 Brussels, Belgium*

Received November 13, 2000; revised January 25, 2001; accepted January 30, 2001; published online May 15, 2001

The kinetics of selective hydrodechlorination of 1,2-dichloroethane into ethylene over a Pd–Ag/SiO_2 catalyst is studied. Kinetic data at 573, 596, and 647 K have been obtained by means of experimental designs in the space of the partial pressures of the four components influencing kinetics, that is, 1,2-dichloroethane, hydrogen, ethylene, and hydrogen chloride. One model among the numerous ones examined allows us to represent correctly the experimental data. It corresponds to the following mechanism: dechlorination of 1,2-dichloroethane into ethylene occurs on silver through dissociative adsorption with successive breaking of the two C–Cl bonds and desorption of C_2H_4. Thanks to its activation power of hydrogen by dissociative chemisorption, palladium present at the surface of the alloy supplies hydrogen atoms for regeneration of the chlorinated silver surface into metallic silver. The presence of hydrogen adsorbed on Pd also causes the undesired ethylene hydrogenation leading to a loss of olefin selectivity. © 2001 Academic Press

Key Words: **hydrodechlorination; 1,2-dichloroethane; Pd–Ag alloys; kinetics; reaction mechanism.**

INTRODUCTION

Hydrodechlorination (HDC) of chlorinated organics is a particularly attractive alternative compared with incineration of wastes from the chlorine industry from both an economical and an environmental point of view (1). Applications of that process to chlorinated alkanes (2–7), chlorinated alkenes (2, 6, 8–10), chlorinated aromatics (6, 11–17), and complex chlorinated molecules (18, 19) can be found in the literature. Hydrodechlorination is also a way for the synthesis of hydro(chloro)fluoro carbons (HCFCs, HFCs) from chlorofluorocarbons (CFCs) (20–28).

In the above-mentioned studies related to chlorinated alkanes and in particular to 1,2-dichloroethane (2), the hydrodechlorination reaction consists always of the carbon–chlorine bond hydrogenolysis, $\equiv C–Cl + H_2 \rightarrow \equiv C–H + HCl$, in which hydrogen atoms are substituted for chlorine atoms. In the case of 1,2-dichloroethane ($ClCH_2–CH_2Cl$), which is studied in the present work, this hydrogenolysis leads to ethane. The catalysts are supported or unsupported monometallic catalysts and metals come essentially from group VIII. The reaction mechanisms generally suggested imply a dissociative adsorption of the chlorinated alkane on the metal surface with successive breakings of C–Cl bonds.

However, recent studies on chlorinated alkanes (29–32) demonstrated the ability of bimetallic catalysts, composed of one metal from group VIII and one from group Ib or chosen among Ga, In, Tl (group IIIa); Ge, Sn, Pb (group IVa); or As, Sb, Bi (group Va), to selectively convert chlorinated alkanes into less or not chlorinated alkenes. This selectivity effect of bimetallic catalysts was also shown in a study of the selective hydrodechlorination of 1,1,2-trichlorotrifluoroethane ($Cl_2FC–CF_2Cl$) into chlorotrifluoroethylene ($ClFC{=}CF_2$) and trifluoroethylene ($HFC{=}CF_2$) on bimetallic catalysts containing palladium and one of the following metals: Cu, Ag (group Ib); Cd, Hg (group IIb); In, Tl (group IIIa); Sn, Pb (group IVa); or Bi (group Va) (33).

The evaluation catalytic tests presented in the first paper of this series (34) demonstrate again this selectivity effect: the hydrodechlorination of $ClCH_2–CH_2Cl$ on a Pd–Ag/SiO_2 bimetallic catalyst produces C_2H_4 to the detriment of C_2H_6 with an ethylene selectivity that increases when the Ag/Pd ratio increases and a similar conclusion is drawn by Vadlamannati *et al.* (35) for Pt–Cu/C catalysts when the Cu/Pt ratio increases.

In the present paper, the selective hydrodechlorination of 1,2-dichloroethane is examined through a kinetic study that has a double purpose. One has first to identify a phenomenological kinetic model that agrees with the experimental rates of reactions involved in the process and, second, to try, thanks to that model but also thanks to the catalyst physicochemical properties detailed in the two previous papers of this series (34, 36) and literature data, to identify as precisely as possible the active sites, the reaction

---

[1] To whom correspondence should be addressed. Fax: +32 4 366 35 45. E-mail: b.heinrichs@ulg.ac.be.

mechanism, and the role played by the palladium–silver alloy.

EXPERIMENTAL

The evaluation catalytic tests presented in the first paper of this series (34) have shown that, among the three bimetallic catalysts tested, that is, Pd–Ag (67-33), Pd–Ag (50-50), and Pd–Ag (33-67) (numbers in brackets refer to the overall atomic composition in the sample), the highest ethylene selectivity was obtained with the catalyst having the highest Ag/Pd ratio, that is, xerogel Pd–Ag (33-67) (1.9% Pd–3.7% Ag/SiO_2). The latter catalyst is then used for the kinetic study of 1,2-dichloroethane hydrodechlorination. Synthesis and characterization of sample Pd–Ag (33-67) are detailed in Refs. (34, 36). In the next section, experimental methods for kinetic data acquisition only are described.

(I) Experimental Device

Reaction rates are measured in a tubular fixed bed reactor. Composition changes between inlet and outlet are sufficiently small so that the reactor is differential (37). To study the effect of all compounds implied in the reaction scheme on reaction rates, it is necessary to introduce at the reactor inlet not only reactants but also the products having an influence on the kinetics. Preliminary tests under various partial pressure and temperature conditions showed that reaction products are composed of ethylene and hydrogen chloride, but also of ethane. At the highest temperatures (596 and 647 K), vinyl chloride ($CH_2{=}CHCl$) is found in traces in the effluent probably because of thermal decomposition of 1,2-dichloroethane (this pyrolysis is at the root of the industrial production of monomer vinyl chloride and is, in that case, performed between 770 and 870 K (38)). However, for the sake of simplification, we have neglected the presence in traces of vinyl chloride in kinetic models. A check of the effect of the three reaction products on the kinetics has then shown that whereas C_2H_4 and HCl have a marked influence on the rates, C_2H_6 has no influence at all. In consequence, the introduction of ethane in the reactor feed is not necessary for the kinetic study.

The feeding section of the kinetic measurement device is composed of four gas lines for H_2, C_2H_4, HCl (diluted in He), and He whose flowrates are adjusted with Brooks mass flowrate controllers. 1,2-Dichloroethane is supplied in liquid phase with a Gilson piston pump. A loop located in the oven upstream from the reactor allows vaporization of $ClCH_2$–CH_2Cl.

The stainless steel tubular reactor with an internal diameter of 8×10^{-3} m and a length of 0.2 m is placed in a convection oven whose temperature is programmed. The temperature within the reactor is measured with a thermocouple slipped into a stainless steel sheath immersed in the catalyst bed. The total pressure is maintained constant via a pressure controller operating a compressed air valve located downstream from the reactor. For all kinetic measurements, the total pressure is fixed at 2.96 atm (0.3 MPa) and the total flowrate is fixed at 0.5 mmol s^{-1}. The temperature within the reactor is fixed successively at 573, 596, and 647 K (see below).

The effluent of the reactor is analyzed by gas chromatography with a Shimadzu GC-14A chromatograph equipped with a 27.5-m Chrompack PoraPLOT capillary column and a flame ionization detector (FID). Although this analysis method theoretically allows measurement of 1,2-dichloroethane, ethylene, and ethane concentrations, only C_2H_4 and C_2H_6 concentrations are used in this study due to the too large imprecision of $ClCH_2$–CH_2Cl concentration measurements.

The 62×10^{-3}-m high catalytic bed is composed of 0.2500×10^{-3} kg of Pd–Ag (33-67) catalyst pellets crushed and sieved between 250×10^{-6} and 500×10^{-6} m. Thus, the minimum ratio between the internal diameter of the reactor and the diameter of the sphere-like pellets is $(8 \times 10^{-3})/(500 \times 10^{-6}) = 16 > 10$. In this case, the influence of the short-circuit along the wall, where the void fraction is higher than that in the core of the bed, on reactor performances is negligible (37).

Prior to the measurement campaign, the catalyst was reduced *in situ* at atmospheric pressure in flowing H_2 (0.025 mmol s^{-1}) while being heated to 623 K at a rate of 350 K h^{-1} and was maintained at this temperature for 3 h.

(II) Measurement of Reaction Rates

Each experiment, which is defined by one temperature and four partial pressures, p_D, p_H, p_E, p_{HCl}, gives two results: net production rate of ethylene r_E and net production rate of ethane r_A. These rates are calculated from chromatographic measurements of C_2H_4 and C_2H_6 concentrations in the reactor effluent and from the differential reactor equation that is written as follows for ethylene and ethane net production:

$$r_E = \frac{F_E - F_{E0}}{W} \quad \text{and} \quad r_A = \frac{F_A}{W} \quad (F_{A0} = 0) \qquad [1]$$

(the meaning of all symbols and units are given in an appendix at the end of the paper).

One hundred twenty experiments, each repeated twice and each yielding two responses, that is, r_E and r_A, were carried out according to one experimental design defined in the space of the four partial pressures having an influence on kinetics (p_D, p_H, p_E, p_{HCl}) and repeated at three temperatures: 573, 596, and 647 K. The partial pressure intervals covered by this experimental design are 0.089 atm $\le p_D \le$ 0.207 atm, 0.089 atm $\le p_H \le$ 0.207 atm, 0.007 atm $\le p_E \le$ 0.025 atm, and

$0.024\ \text{atm} \le p_{\text{HCl}} \le 0.047\ \text{atm}$. All details concerning kinetic data acquisition can be found in Ref. (39).

(III) External and Internal Transfers

According to mass transfer calculations and experimental tests presented in another paper (40) devoted to mass transfer in the Pd–Ag (33-67) xerogel, reaction rate values used in the present kinetic study are not falsified by diffusional limitations. Thus, those values reflect the intrinsic chemical kinetics. It is shown in Ref. (40) that cogelled xerogel catalysts like Pd–Ag (33-67) exhibit remarkable mass transfer properties.

Under reaction conditions used in this study, external and internal heat transfer are also negligible. Indeed, the 1,2-dichloroethane hydrodechlorination into ethylene is a quasiathermal reaction (reaction standard enthalpy at 600 K, $-5\ \text{J mmol}^{-1}$). On the other hand, ethylene hydrogenation is highly exothermic (reaction standard enthalpy at 600 K, $-142\ \text{J mmol}^{-1}$), but, thanks to the selectivity of the Pd–Ag (33-67) catalyst, this hydrogenation is very limited.

RESULTS

(I) Experimental Data

The reaction scheme examined in this study implies *a priori* the reactions

$$\begin{aligned} &\text{ClCH}_2\text{–CH}_2\text{Cl} + \text{H}_2 \rightarrow \text{CH}_2{=}\text{CH}_2 + 2\text{HCl} &&\text{rate } r_1\\ &\text{CH}_2{=}\text{CH}_2 + \text{H}_2 \rightarrow \text{CH}_3\text{–CH}_3 &&\text{rate } r_2\\ &\text{ClCH}_2\text{–CH}_2\text{Cl} + 2\text{H}_2 \rightarrow \text{CH}_3\text{–CH}_3 + 2\text{HCl} &&\text{rate } r_3,\end{aligned}$$

which correspond to the consecutive-parallel reaction scheme given in Fig. 1. In the temperature domain examined here ($573\ \text{K} \le T \le 647\ \text{K}$), equilibrium constants of these three reactions are very high: $1.5 \times 10^8 \le K_{\text{reaction 1}} \le 1.7 \times 10^8$; $3.5 \times 10^4 \le \text{K}_{\text{reaction 2}} \le 1.0 \times 10^6$; $K_{\text{reaction 3}} = K_{\text{reaction 1}} K_{\text{reaction 2}}$. Therefore, the three reactions can be considered as irreversible reactions.

The consumption rate of 1,2-dichloroethane and the production rate of ethane are obtained via mass balances:

$$r_1 + r_3 = r_{\text{E}} + r_{\text{A}} \quad \text{ClCH}_2\text{–CH}_2\text{Cl consumption} \quad [2]$$

$$r_2 + r_3 = r_{\text{A}} \quad \text{C}_2\text{H}_6 \text{ production.} \quad [3]$$

Experimental values of these rates obtained through the above-mentioned experimental design were corrected with regard to the catalyst deactivation so as to all correspond to the same activity level[2]. The correction procedure consists of measuring the consumption rate of 1,2-dichloroethane, $r_{\text{E}} + r_{\text{A}}$, and the production rate of ethane, r_{A}, regularly under reference conditions that correspond to the center of the experimental design described above. Between two consecutive sets of rates measured under those reference conditions, it can be considered that deactivation is linear and a linear deactivation function is fitted on rate values contained in the two reference sets (37). Rate values located between those two reference sets are then corrected by means of the linear deactivation function which allows them to be restored to an initial activity level. This level corresponds to the catalyst activity at the beginning of the experimental design run. All details concerning the correction procedure can be found in Ref. (39). The causes of the deactivation observed will be examined in the next paper of this series.

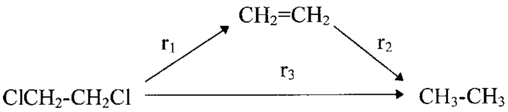

FIG. 1. Consecutive-parallel reaction scheme.

(II) Parameter Estimation and Statistical Testing of Models

The fitting of kinetic models was performed by applying the Gauss–Newton optimization method to the minimization of the experimental chi-square function (41, 42). NLPE software, Non Linear Parameter Estimation, from IBM was used. The adequacy of the various models examined to the experimental data was tested by means of a chi-square test (41, 42). All details concerning parameter estimation and statistical tests can be found in Ref. (39).

(III) Reaction Mechanism and Kinetic Equations

Empirical model: power rate laws. *A priori*, numerous kinetic equations corresponding to well-defined sequences of elementary steps and rate determining steps can be imagined so as to try to model experimental data. To restrict the number of plausible candidates among phenomenological kinetic models, the apparent reaction orders in 1,2-dichloroethane, hydrogen, ethylene, and hydrogen chloride are first examined by means of an empirical model, the two equations of which are power rate laws

$$\begin{aligned} r_1 + r_3 &= k_1 p_{\text{D}}^{w_1} p_{\text{H}}^{x_1} p_{\text{E}}^{y_1} p_{\text{HCl}}^{z_1}\\ r_2 + r_3 &= k_2 p_{\text{D}}^{w_2} p_{\text{H}}^{x_2} p_{\text{E}}^{y_2} p_{\text{HCl}}^{z_2}. \end{aligned} \quad [4]$$

The meaning of rates r_1, r_2, and r_3 is given in Fig. 1. In the particular case of this power law model, parameter estimation has been performed separately at each temperature. Values of the 10 parameters of this model with their 95% confidence intervals are given in Table 1 for each temperature. The chi-square test indicates that the empirical model represents correctly the experimental data at each temperature separately. The examination of values obtained

---

[2] The data set was too extensive to be incorporated in full in the text. It is available from the corresponding author.

TABLE 1

Parameter Estimation Results for the Empirical Power Rate Law Model

Parameters	573 K	596 K	647 K
k_1	0.79 ± 0.76	3.3 ± 1.5	3.1 ± 2.8
w_1	0.91 ± 0.18	0.96 ± 0.09	0.70 ± 0.17
x_1	0.46 ± 0.16	0.25 ± 0.07	0.25 ± 0.15
y_1	-0.11 ± 0.11	-0.07 ± 0.05	-0.47 ± 0.11
z_1	-0.92 ± 0.22	-0.67 ± 0.10	-0.31 ± 0.19
k_2	9.6 ± 3.6	8.8 ± 8.1	12.1 ± 7.6
w_2	-0.04 ± 0.05	0.16 ± 0.12	-0.17 ± 0.08
x_2	1.59 ± 0.08	1.83 ± 0.21	1.76 ± 0.15
y_2	1.01 ± 0.06	0.83 ± 0.12	0.86 ± 0.09
z_2	-0.91 ± 0.07	-1.09 ± 0.19	-0.89 ± 0.12

Note. Reaction rate units are mmol kg^{-1} s^{-1} and partial pressure units are atm.

for the apparent reaction orders with their confidence intervals shows that

$r_1 + r_3$ is
- quasi first order in $ClCH_2$–CH_2Cl at the three temperatures (w_1)
- positive and decreasing with temperature order in H_2 (x_1)
- negative and decreasing with temperature order in C_2H_4 (y_1)
- negative and increasing with temperature order in HCl (z_1)

$r_2 + r_3$ is
- quasi independent of $ClCH_2$–CH_2Cl pressure (order ≈ 0)(w_2)
- between 1.5 and 2nd order in H_2 (x_2)
- first or slightly lower order in C_2H_4 (y_2)
- close to -1 order in HCl (z_2)

The ethane production rate $r_2 + r_3$ is virtually independent of the 1,2-dichloroethane partial pressure which could indicate that $ClCH_2$–CH_2Cl plays no role in C_2H_6 production. Hence, ethane would be produced almost exclusively through ethylene hydrogenation; i.e., rate r_3 would be negligible in comparison with r_2 (Fig. 1). The consecutive-parallel reaction scheme in Fig. 1 would then simplify to the consecutive reaction scheme

$$ClCH_2\text{–}CH_2Cl \xrightarrow{r_1} CH_2{=}CH_2 \xrightarrow{r_2} CH_3\text{–}CH_3$$

or more explicitly to

$$\begin{array}{ll} ClCH_2\text{–}CH_2Cl + H_2 \rightarrow CH_2{=}CH_2 + 2HCl & \text{rate } r_1 \\ CH_2{=}CH_2 + H_2 \rightarrow CH_3\text{–}CH_3 & \text{rate } r_2. \end{array}$$

Phenomenological kinetic models corresponding to this scheme and their adequacy to experimental data are examined below. The two consecutive reactions are called hydrodechlorination reaction (rate r_1) and hydrogenation reaction (rate r_2), respectively.

Phenomenological models. To try to identify one or several models that are able to describe correctly the kinetic data, various equations were examined successively. A sequence of elementary steps describing the catalytic mechanism and two rate-determining steps, one for hydrodechlorination (rds1) and one for hydrogenation (rds2), were assumed and rate equations were deduced. Parameters of these equations were next estimated and the quality of the model was evaluated by means of the chi-square test on the one hand and by examining its compatibility with apparent orders in Table 1 on the other hand. On the basis of this evaluation, models were progressively improved by modifying the sequence of elementary steps. In this way, twenty models were examined. Those models were based on various choices concerning the two rate-determining steps (rds) and various hypotheses such as the presence of one or two types of active sites, molecular or dissociative adsorption of the compounds influencing the kinetics (1,2-dichloroethane, hydrogen, ethylene, and hydrogen chloride), surface reactions between adsorbed species only (Langmuir–Hinshelwood kinetics) or between adsorbed species and molecules in the gas phase (Eley–Rideal kinetics), and the type of sites on which each species is adsorbed when two types are considered. Among the 20 models considered, only one describes correctly the whole set of kinetic data according to the chi-square test. This model is based on a Langmuir–Hinshelwood mechanism involving two types of active sites, s_1 and s_2. The corresponding sequence of elementary steps is presented below (Sequence [5]).

Hydrodechlorination

$$\begin{array}{llcllll}
 & & & & \underline{\sigma} & \\
1. & ClCH_2CH_2Cl + 2s_1 & \rightarrow & ClCH_2CH_2s_1 + Cls_1 & 1 & \text{rds1}: r_1 = k_1' p_D [s_1]^2 \\
2. & ClCH_2CH_2s_1 + s_1 & \leftrightarrow & C_2H_4s_1 + Cls_1 & 1 & K_2 = \frac{[C_2H_4s_1][Cls_1]}{[ClCH_2CH_2s_1][s_1]} \\
3. & C_2H_4s_1 & \leftrightarrow & C_2H_4 + s_1 & 1 & K_3 = \frac{[C_2H_4s_1]}{p_E[s_1]} \\
4. & H_2 + 2s_2 & \leftrightarrow & 2Hs_2 & 1 & K_4 = \frac{[Hs_2]^2}{p_H[s_2]^2} \\
5. & Hs_2 + Cls_1 & \leftrightarrow & HCl + s_2 + s_1 & 2 & K_5 = \frac{[Hs_2][Cls_1]}{p_{HCl}[s_2][s_1]} \\
\hline
\multicolumn{2}{l}{ClCH_2CH_2Cl + H_2} & \rightarrow & C_2H_4 + 2HCl & &
\end{array} \qquad [5]$$

Hydrogenation

$$\begin{array}{llcllll}
 & & & & \underline{\sigma} & \\
3. & C_2H_4 + s1 & \leftrightarrow & C_2H_4s_1 & 1 & K_3 \\
4. & H_2 + 2s_2 & \leftrightarrow & 2Hs_2 & 1 & K_4 \\
6. & C_2H_4s_1 + Hs_2 & \leftrightarrow & C_2H_5s_1 + s_2 & 1 & K_6 = \frac{[C_2H_4s_1][Hs_2]}{[C_2H_5s_1][s_2]} \\
7. & C_2H_5s_1 + Hs_2 & \rightarrow & C_2H_6 + s_1 + s_2 & 1 & \text{rds2}: r_2 = k_2'[C_2H_5s_1][Hs_2] \\
\hline
\multicolumn{2}{l}{C_2H_4 + H_2} & \rightarrow & C_2H_6 & &
\end{array}$$

Exchange of adsorbed chlorine atoms between s_1 and s_2

$$\begin{array}{llclll}
8. & Cls_1 + s_2 & \leftrightarrow & Cls_2 + s_1 & & K_8 = \frac{[Cls_2][s_1]}{[Cls_1][s_2]}
\end{array}$$

The addition of elementary steps involved in hydrodechlorination or in hydrogenation, each one being multiplied by a relevant factor called the stoichiometric number

σ, leads to the overall stoichiometric equation. The steps determining the rates of hydrodechlorination and hydrogenation, rds1 and rds2, are the elementary reactions 1 and 7. Since the overall reactions are irreversible in the temperature domain studied here (see above), these two rds are also irreversible. Steps 2 to 6 and step 8 are considered to be in a quasi-equilibrium characterized by an equilibrium constant K_i (43, 44). Note that, when describing an adsorption–desorption quasi-equilibrium, constants K_i are always written as adsorption constants.

In Sequence [5], the majority of species are adsorbed on sites s_1 except for hydrogen which is dissociatively adsorbed on sites s_2 and chlorine atoms which are adsorbed on both s_1 and s_2. Step 8 corresponds to a spillover from sites s_1 to sites s_2 of chlorine atoms initially adsorbed on sites s_1 via steps 1, 2, and 5. Step 8 is not directly involved in the reactions but is necessary so as to describe correctly the very strong inhibiting effect of HCl on ethylene hydrogenation (order z_2 in HCl close to -1, see Table 1) whose rate-determining step rds2 involves both s_1 and s_2.

By means of balances expressing that the total number of active sites of each type is constant, kinetic Equations [6] corresponding to Sequence [5] are obtained (43). The total concentrations in active sites s_1 and s_2 are determined to be equal to 1; i.e., their values are simply absorbed in the rate constants k_1 and k_2 (45). Let us mention that some adsorption terms are omitted in Equations [6] since they are negligible according to preliminary parameter estimations. Those terms are $C p_{\mathrm{E}} = \frac{[\mathrm{C_2H_4}s_1]}{[s_1]}$ with $C = K_3$, $E p_{\mathrm{E}}\sqrt{p_{\mathrm{H}}} = \frac{[\mathrm{C_2H_5}s_1]}{[s_1]}$ with $E = \frac{K_3\sqrt{K_4}}{K_6}$, and $D\sqrt{p_{\mathrm{H}}} = \frac{[\mathrm{H}s_2]}{[s_2]}$ with $D = \sqrt{K_4}$.

$$r_1 = \frac{k_1 p_{\mathrm{D}}}{\left(1 + A\frac{p_{\mathrm{E}} p_{\mathrm{HCl}}}{\sqrt{p_{\mathrm{H}}}} + B\frac{p_{\mathrm{HCl}}}{\sqrt{p_{\mathrm{H}}}}\right)^2} \quad \text{Hydrodechlorination}$$

$$[6]$$

$$r_2 = \frac{k_2 p_{\mathrm{E}} p_{\mathrm{H}}}{\left(1 + A\frac{p_{\mathrm{E}} p_{\mathrm{HCl}}}{\sqrt{p_{\mathrm{H}}}} + B\frac{p_{\mathrm{HCl}}}{\sqrt{p_{\mathrm{H}}}}\right)\left(1 + F\frac{p_{\mathrm{HCl}}}{\sqrt{p_{\mathrm{H}}}}\right)} \quad \text{Hydrogenation}$$

with

$$k_1 = k_1'; \quad k_2 = k_2'\frac{K_3K_4}{K_6}; \qquad [7]$$
$$A = \frac{K_3K_5}{K_2\sqrt{K_4}}; \quad B = \frac{K_5}{\sqrt{K_4}}; \quad F = \frac{K_5K_8}{\sqrt{K_4}}.$$

The three adsorption terms in the denominator of r_1 and r_2 correspond to the following adsorbed species:

$$A\frac{p_{\mathrm{E}} p_{\mathrm{HCl}}}{\sqrt{p_{\mathrm{H}}}} = \frac{[\mathrm{ClCH_2CH_2}s_1]}{[s_1]}; \; B\frac{p_{\mathrm{HCl}}}{\sqrt{p_{\mathrm{H}}}} = \frac{[\mathrm{Cl}s_1]}{[s_1]};$$

$$[8]$$

$$F\frac{p_{\mathrm{HCl}}}{\sqrt{p_{\mathrm{H}}}} = \frac{[\mathrm{Cl}s_2]}{[s_2]}.$$

Thus, only species $\mathrm{ClCH_2CH_2}$- and Cl- are present in significant amounts on site s_1, whereas on site s_2 only Cl- is significantly present.

In sequences of elementary steps like Sequence [5], it is generally admitted that rate constants k_1' and k_2' depend on temperature according to Arrhenius' law and that equilibrium constants K_i follow van't Hoff's law (46). Therefore, according to Eqs. [7], parameters k_1, k_2, A, B and F in Equations [6] can be written as

$$k_1 = k_{1,\mathrm{ref}} \exp\left[-\frac{E_1}{R}\left(\frac{1}{T} - \frac{1}{T_{\mathrm{ref}}}\right)\right]$$
$$\text{with} \quad k_{1,\mathrm{ref}} = k_{01}\exp\left(-\frac{E_1}{RT_{\mathrm{ref}}}\right)$$
$$k_2 = k_{2,\mathrm{ref}} \exp\left[-\frac{E_2}{R}\left(\frac{1}{T} - \frac{1}{T_{\mathrm{ref}}}\right)\right]$$
$$\text{with} \quad k_{2,\mathrm{ref}} = k_{02}\exp\left(-\frac{E_2}{RT_{\mathrm{ref}}}\right)$$
$$A = A_{\mathrm{ref}} \exp\left[-\frac{\Delta H_{\mathrm{A}}^0}{R}\left(\frac{1}{T} - \frac{1}{T_{\mathrm{ref}}}\right)\right] \qquad [9]$$
$$\text{with} \quad A_{\mathrm{ref}} = A_0\exp\left(-\frac{\Delta H_A^0}{RT_{\mathrm{ref}}}\right)$$
$$B = B_{\mathrm{ref}} \exp\left[-\frac{\Delta H_{\mathrm{B}}^0}{R}\left(\frac{1}{T} - \frac{1}{T_{\mathrm{ref}}}\right)\right]$$
$$\text{with} \quad B_{\mathrm{ref}} = B_0\exp\left(-\frac{\Delta H_B^0}{RT_{\mathrm{ref}}}\right)$$
$$F = F_{\mathrm{ref}} \exp\left[-\frac{\Delta H_{\mathrm{F}}^0}{R}\left(\frac{1}{T} - \frac{1}{T_{\mathrm{ref}}}\right)\right]$$
$$\text{with} \quad F_{\mathrm{ref}} = F_0\exp\left(-\frac{\Delta H_F^0}{RT_{\mathrm{ref}}}\right)$$

with

$$k_{01} = k_{01}'; \; E_1 = E_{\mathrm{a1}}$$
$$k_{02} = k_{02}'\frac{K_{03}K_{04}}{K_{06}}; \; E_2 = E_{\mathrm{a2}} + \Delta H_3^0 + \Delta H_4^0 - \Delta H_6^0$$
$$A_0 = \frac{K_{03}K_{05}}{K_{02}\sqrt{K_{04}}}; \; \Delta H_A^0 = \Delta H_3^0 + \Delta H_5^0 - \Delta H_2^0$$
$$- \frac{1}{2}\Delta H_4^0 \qquad [10]$$
$$B_0 = \frac{K_{05}}{\sqrt{K_{04}}}; \; \Delta H_{\mathrm{B}}^0 = \Delta H_5^0 - \frac{1}{2}\Delta H_4^0$$
$$F_0 = \frac{K_{05}K_{08}}{\sqrt{K_{04}}}; \; \Delta H_{\mathrm{F}}^0 = \Delta H_5^0 + \Delta H_8^0 - \frac{1}{2}\Delta H_4^0.$$

T_{ref} is a reference temperature fixed to an intermediate value in the temperature domain under consideration (41, 46).

Parameter estimation with all the kinetic data was performed with Equations [6] in which the temperature

TABLE 2

Parameter Estimation Results for the Phenomenological Model Based on Eqs. [6] and [9]

Parameters		Values
$k_1 = k'_1$	$k_{1,\mathrm{ref}}$	61.7 ± 6.7
	E_1	49.1 ± 9.2
$k_2 = k'_2 \frac{K_3 K_4}{K_6}$	$k_{2,\mathrm{ref}}$	637 ± 174
	E_2	74.2 ± 24.0
$A = \frac{K_3 K_5}{K_2 \sqrt{K_4}}$	A_{ref}	58.1 ± 24.4
	ΔH^0_{A}	68.6 ± 33.3
$B = \frac{K_5}{\sqrt{K_4}}$	B_{ref}	3.5 ± 0.8
	ΔH^0_{B}	−73.0 ± 16.3
$F = \frac{K_5 K_8}{\sqrt{K_4}}$	F_{ref}	34.7 ± 13.3
	ΔH^0_{F}	68.8 ± 27.7

Note. Reaction rate units are mmol $\mathrm{kg}^{-1}\,\mathrm{s}^{-1}$ and partial pressure units are atm.

dependence of constants k_1, k_2, A, B, and F is expressed via relations [9] with $T_{\mathrm{ref}} = 600$ K. Results are given in Table 2. As mentioned above, Model [6] satisfies the chi-square test.

Let us mention that among the other 19 phenomenological models tested, two models greatly contributed to the construction of Sequence [5] of elementary steps and its associated equations [6]. The first of those two models is based on a sequence consisting of the first seven steps of Sequence [5] but in which only one type of active site is involved. In other words, the sequence corresponding to that model is Sequence [5] (except step 8) in which $s_1 = s_2 = s$. That model was rejected by the chi-square test. As a consequence of this rejection, a second model based on a similar sequence but that now involves two types of active sites, s_1 and s_2, was considered. That second model corresponds to a sequence composed of the same eight steps as those in Sequence [5], but in which ethylene C_2H_4 and alkyl fragment -C_2H_5 are adsorbed on sites s_2 instead of sites s_1. Therefore, in that model, all species involved in ethylene hydrogenation are adsorbed on sites s_2 and the rate-determining step for ethylene hydrogenation rds2 involves two sites s_2 instead of one site s_1 and one site s_2. Once again that second model was rejected by the chi-square test. This result led us to construct the only model accepted by the chi-square test and which is based on Sequence [5] and Equations [6].

According to results presented in this section, among 20 kinetic models tested, only the model corresponding to Sequence [5] of elementary steps is statistically satisfactory. This model suggests the existence of two types of active sites involved in the hydrodechlorination–hydrogenation system. In the discussion below, we examine the physicochemical validity of that model as well as the nature of the active sites s_1 and s_2 in light of the literature data.

DISCUSSION

The breaking of carbon–halogen bonds was examined on various metals. According to the study of Fung and Sinfelt concerning the hydrogenolysis of methyl chloride CH_3Cl on metals (5), the ability of metals from group Ib such as Ag to form a metal–chlorine bond, as demonstrated by the existence of stable chlorides, allows the chemisorption of chlorinated molecules such as CH_3Cl and the associated breaking of the C–Cl bond. In the case of methyl iodide CH_3I (47, 48), the C–I bond dissociates more easily on copper (metal from group Ib like Ag) than on platinum (metal from group VIII like Pd). In a study of dehalogenation, without hydrogen, of haloethanes and halopropanes with metals supported on silica, Anju *et al.* (49) measured at 573 K a dechlorination rate of 1,2-dichloroethane into ethylene that was 13 times higher on silver than on palladium.

In Sequence [5] of elementary steps corresponding to the kinetic model [6], the steps that describe dissociative adsorption of 1,2-dichloroethane with successive breakings of the two C–Cl bonds (steps 1 and 2) occur on sites s_1. According to literature results cited above, those sites s_1 could then be silver sites.

To measure the various dehalogenation rates and particularly the dechlorination rate of 1,2-dichloroethane into ethylene on supported metals, among them Pd and Ag, Anju *et al.* (49) used a pulse microcatalytic technique that consists of sending a pulse of haloalkane on the catalyst and measuring activity from the fraction of haloalkane converted, conversion being maintained under 20%. With this technique, the authors have shown that activity decreases pulse after pulse. Conversion corresponding to the second pulse is divided by around two in comparison with conversion corresponding to the first pulse. According to Anju *et al.* (49), this deactivation means that the reaction under consideration consists of the halogenation of the metals by the haloalkanes. This observation is supported and greatly clarified by the work of Yang (47) who studied the dechlorination of chloroethanes, among them 1,2-dichloroethane, and of chloropropanes containing several chlorine atoms over the cristallographic plane (100) of copper under ultrahigh vacuum between 100 and 300 K by Auger electron spectroscopy and temperature programmed desorption. In those molecules, the breaking of C–Cl bonds is always favored in relation to the breaking of C–H bonds, which was previously observed with various chlorinated alkanes (3, 4). In the case of 1,2-dichloroethane and 1,2-dichloropropane ($ClCH_2$–$ClCH$–CH_3), dechlorination occurs in two successive steps: a first slow step that determines the rate of the overall dissociative adsorption process and that consists of the breaking of the first C–Cl bond followed by a second fast step consisting of the breaking of the second C–Cl bond and the desorption of ethylene or propylene. It is very interesting to note that this process described by Yang for dechlorination on copper corresponds exactly to Sequence [5] of the present study, specifically to steps 1, 2 and 3 occurring on sites s_1 identified with silver sites: a first step, which is the slow step of the process, consisting of the dissociative adsorption of 1,2-dichloroethane on sites s_1 with the breaking of a first C–Cl bond, a second step consisting of the breaking of a second C–Cl bond, and a third step consisting of the desorption of ethylene adsorbed on sites s_1.

By considering, in Sequence [5], step 2 characteristic of hydrodechlorination, step 3 occurring in both hydrodechlorination and hydrogenation, and step 6 characteristic of hydrogenation, the identification of sites s_1 with silver raises the question of the possibility of ethylene adsorbing on this metal. Literature concerning ethylene epoxidation, $C_2H_4 + 1/2O_2 \rightarrow C_2H_4O$ ($T \approx 500$ K), over silver is particularly useful in answering this question. Wachs and Kelemen (50) showed that above 200 K, ethylene almost does not adsorb on a clean (110) Ag surface and this absence of adsorption of C_2H_4 on clean metallic silver is mentioned by numerous other authors (51–55). However, the presence of oxygen atoms at the surface of silver causes ethylene adsorption and it seems that this adsorption occurs selectively on silver atoms on which a positive electric charge has been induced by the neighboring electronegative adsorbed oxygen atoms (56–58). In a more general manner, the strength of the Ag–C_2H_4 bond increases with the electrodeficient character of silver. For example, Huang (59) showed that at 298 K ethylene is strongly adsorbed on Ag^+ cations incorporated in a zeolite structure. Let us remark that the same effect was observed on Cu^+ and Cu^{2+} ions (59–61). Olefin adsorption results from the interaction of electrophilic Ag^+ with electrons of its double bond. In the case of ethylene epoxidation, the oxygen atoms that are initially adsorbed on the external surface of silver following O_2 dissociation can migrate and occupy a position located just under the surface and continue, from this position, to induce Ag^+ ions at the surface on which ethylene can adsorb (57, 62). This occupation of sites just under the surface results from diffusion of adsorbed atomic oxygen that occurs above 373 K (63). Like oxygen atoms, chlorine atoms adsorbed on the surface induce, following their electronegativity, positive charges on the neighboring silver atoms and, thanks to their ability to also adsorb under the surface, they can play the same role as the corresponding oxygen atoms (62). As a consequence, it appears that, in the kinetic model presented in the previous section, ethylene adsorption on silver is entirely plausible following the presence of chlorine atoms adsorbed on that metal. Such an adsorption is schematically represented in Fig. 2. Let us remark that, in their study on the interaction between oxygen and ethylene on silver, Kagawa *et al.* (58) conclude that oxygen not only induces $Ag^{\delta+}$ sites, but also competes, as ethylene oxide, with ethylene for adsorption on these positively charged sites. This result is qualitatively in agreement with the hypothesis of competitive adsorption of the various species on sites s_1 in the kinetic model corresponding to Sequence [5] ($ClCH_2CH_2s_1$, Cls_1, $C_2H_4s_1$, and $C_2H_5s_1$).

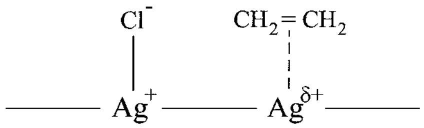

FIG. 2. Schematic representation of ethylene adsorption on silver in presence of chlorine.

Let us now examine sites s_2. According to step 4 in Sequence [5], it is plausible to assimilate sites s_2 to palladium sites. Indeed, dissociative adsorption of hydrogen is well known on that metal according to reaction $H_2 + 2Pd_s \rightarrow 2Pd_s$–H ($Pd_s$ represents a surface atom), which is particularly used for palladium dispersion measurements by means of hydrogen chemisorption (64). However, according to the work of Nieuwenhuys *et al.* (65, 66), the vast majority of palladium atoms at the surface of Pd–Ag bimetallic particles in fresh Pd–Ag (33-67) catalyst would be individually isolated (36). In such a case, is H_2 dissociative adsorption still possible? In a detailed study of the interaction, between 250 and 500 K, of hydrogen with a Pd–Ag (111) surface whose approximate composition was 10% Pd–90% Ag, that is, a surface composition entirely similar to the one in fresh Pd–Ag (33-67) catalyst (36), Noordermer *et al.* (67) come to the conclusion that isolated palladium atoms on that surface are effectively able to dissociate the hydrogen molecule and that this process is a first step that is followed by the diffusion of H atoms in the bulk of the Pd–Ag crystal. This study of Noordermeer *et al.* (67) shows then that step 4 in Sequence [5] is physically acceptable.

If one accepts the hypothesis according to which $s_1 \equiv$ Ag and $s_2 \equiv$ Pd, step 5 in Sequence [5] shows clearly the role played by palladium in the alloy: thanks to its ability to activate hydrogen through dissociative adsorption that metal supplies the H atoms necessary for the reduction of Ag–Cl at the surface and the regeneration into metallic silver which is not able itself to activate H_2 (44, 68). Without palladium, chlorine would quickly deactivate silver by recovering its surface. This explains the complete inactivity of silver in the stationary regime during the evaluation tests of various catalysts (34).

In conclusion, it appears then that the various steps of the mechanism suggested for the hydrodechlorination reaction in the model associated with Sequence [5], which is statistically acceptable (see previous section), are in agreement with results obtained in other studies.

Concerning ethylene hydrogenation in Sequence [5], steps 3, 4, 6, and 7 with the latter as rds correspond to an additive mechanism of atomic hydrogen to noncompetitively adsorbed ethylene in two successive steps. According to the identification of active sites presented above, ethane production would then result from the addition of H atoms adsorbed on palladium to the C_2H_4 molecule adsorbed on positively charged silver ($Ag^{\delta+}$). Let us remark that such a mechanism is similar to the results obtained by Pirard *et al.* (60, 61, 69) in a study of ethylene hydrogenation over a Cu/MgO catalyst between 326 and 550 K. Kinetic measures coupled with an analysis of the copper (II) ion in the course of reaction by electron spin resonance (ESR) led those authors to the following conclusions: (i) hydrogen and ethylene adsorb noncompetitively; (ii) ethylene is adsorbed on Cu^{2+} surface cations and hydrogen adsorbs on O^{2-} anions coordinated to Cu^{2+}. Although the catalyst and the reaction system are different in that work compared with the present study, it is interesting to note that an adsorption of C_2H_4 on a positively charged metallic species and a noncompetitive adsorption of H_2 are proposed in the two studies.

In the Sequence [5] of elementary steps, step 8 corresponding to an exchange of adsorbed chlorine atoms between sites s_1 and s_2 accounts for the blocking of sites s_2 by Cl atoms. According to the site identification, this step corresponds to a spillover of chlorine atoms formed on silver toward palladium. Let us remark that spillover from one metal to an other has been observed with hydrogen atoms on alloys such as Ru–Cu, Ru–Ag, Ru–Au, and Pt–Au (70).

Let us now examine the values obtained for the hydrodechlorination and hydrogenation activation energies as well as for the reaction enthalpies associated with elementary steps in quasi-equilibrium.

In their study on the dehalogenation of haloalkanes, Anju *et al.* (49) determined the activation energies associated with the dechlorination of 1,2-dichloroethane on silver and on palladium by means of an Arrhenius plot giving the logarithm of the reaction rate versus the inverse of the temperature. If it is admitted that in that study the slow step that governs the kinetics of the overall catalytic process is also the breaking of the first C–Cl bond, the pulse microcatalytic method used by Anju *et al.* (49) supplies an estimation of the intrinsic activation energy of that step. Since the value of E_1 calculated from the model associated with Sequence [5] reflects also the intrinsic activation energy of the first C–Cl breaking (Sequence [5] and Equations [6], [7], and [9]), the value obtained by Anju *et al.* (49) can be compared with the one obtained here. Although, according to those authors, silver is much more active than palladium for dechlorination of 1,2-dichloroethane, the activation energies determined with those two metals are equal and are 53 J $mmol^{-1}$. It is remarkable to note that the value $E_1 = 49 \pm 9$ J $mmol^{-1}$ found in the present study (Table 2) is in complete agreement with the value of Anju *et al.* (49).

On metals from group VIII, the activation energy of ethylene hydrogenation most of the time is contained between 30 and 45 J $mmol^{-1}$ (71, 72). Those values were determined at very different temperatures contained between 153 and 873 K. In the particular case of palladium, values of 35 J $mmol^{-1}$ (for temperatures around 243 K), 31 J $mmol^{-1}$ ($343\,K \le T \le 403\,K$), and 23 J $mmol^{-1}$ ($273\,K \le T \le 373\,K$) were reported. On silver, a much higher activation energy of 113 J $mmol^{-1}$ was obtained for ethylene hydrogenation between 823 and 973 K (72). It is then noted that the activation energy $E_2 = 74 \pm 24$ J $mmol^{-1}$ obtained with the present kinetic model (Equations [6] and [9], Table 2) and which corresponds to a reaction involving both palladium and silver is contained between the values obtained with the two metals separately. However, it is important to remark that, contrary to the case of 1,2-dichloroethane dechlorination in Ref. (49), the various values given in Refs. (71) and (72) for ethylene hydrogenation activation energy correspond to apparent activation energies for two reasons: (i) they are often obtained by means of power law empirical models of the type $r = kp_H^x p_E^y$, which are valid in a limited temperature domain only and they are in such a case dependent on reaction conditions; (ii) they represent combinations of the true activation energy with enthalpy changes associated with various elementary steps of the overall hydrogenation process. Consequently, the comparison of the values of ethylene hydrogenation activation energy given in Refs. (71) and (72) with the value $E_2 = 74 \pm 24$ J $mmol^{-1}$ (Table 2) corresponding also to an apparent activation energy given by $E_2 = E_{a2} + \Delta H_3^0 + \Delta H_4^0 - \Delta H_6^0$ (Equations [10]) must be made for information only.

As in the case of the apparent activation energy E_2, the detailed physicochemical interpretation of the values obtained for ΔH_A^0, ΔH_B^0, and ΔH_F^0 (Table 2) in relation to the various elementary steps is difficult because those parameters correspond to combinations of enthalpy changes: $\Delta H_A^0 = \Delta H_3^0 + \Delta H_5^0 - \Delta H_2^0 - 1/2\Delta H_4^0$, $\Delta H_B^0 = \Delta H_5^0 - 1/2\Delta H_4^0$ and $\Delta H_F^0 = \Delta H_5^0 + \Delta H_8^0 - 1/2\Delta H_4^0$ (Equation [10]). Expressions of ΔH_B^0 and ΔH_F^0 show that it is, however, possible to calculate ΔH_8^0 which corresponds to the enthalpy change associated with the spillover of adsorbed chlorine atoms from sites s_1 to sites s_2: $\Delta H_8^0 = \Delta H_F^0 - \Delta H_B^0$. With the values of ΔH_B^0 and ΔH_F^0 given in Table 2 ($\Delta H_B^0 = -73$ J $mmol^{-1}$ and $\Delta H_F^0 = 69$ J $mmol^{-1}$), one obtains $\Delta H_8^0 = 142$ J $mmol^{-1}$. This positive enthalpy change leads to the conclusion that the spillover of Cl from s_1 to s_2 would be an endothermic process and, thus, that species Cls_1 would be more stable than species Cls_2. Knowing that s_1 and s_2 are identified with silver and palladium, respectively, chlorine would thus be more strongly linked with silver than with palladium.

To end the present physicochemical analysis of the kinetic model based on the Sequence [5] of elementary steps, an important remark must still be formulated. In the above discussion, considerations concerning pure palladium and pure silver are often applied to the same metal dispersed in the Pd–Ag alloy. Such an approach assumes implicitly that, in this alloy, the two metals keep their own properties.

In other words, the electronic effect, also called the ligand effect, of silver on palladium and *vice versa* is assumed to be negligible. According to Sachtler (73), this hypothesis is acceptable for alloys exhibiting a low heat of formation, that is, alloys forming a continuous series of solid solutions in the whole domain of composition, which is effectively the case for the Pd–Ag alloy (74).

CONCLUSIONS

From the statistical point of view, the kinetic model derived from Sequence [5] of elementary steps correctly represents the whole kinetic data. Moreover, it appears from the above discussion that this model is acceptable from a physicochemical point of view and is in agreement with results obtained by other authors. Accordingly, we propose it as a plausible candidate for the description of the catalytic phenomena occurring at the surface of bimetallic Pd–Ag crystallites in the hydrodechlorination–hydrogenation system.

The kinetics of 1,2-dichloroethane hydrodechlorination over the Pd–Ag (33-67) (1.9% Pd–3.7% Ag/SiO_2) catalyst between 573 and 647 K is satisfactorily described by Equations [6]. In those equations, the rate r_1 corresponds to the selective hydrodechlorination of 1,2-dichloroethane into ethylene and the rate r_2 corresponds to the undesired subsequent hydrogenation of ethylene into ethane. Parameters k_1, k_2, A, B, and F in those equations represent groups of kinetic and equilibrium constants defined by Relations [7] and their temperature dependency is given by Equations [9] and [10].

That model is based on the Sequence [5] of elementary steps which suggests a process of chlorination of the silver surface by the chlorinated alkane followed by a hydrodechlorination of that surface by hydrogen adsorbed on palladium. This situation is illustrated in Fig. 3. Therefore, the roles played by silver and palladium in the catalytic process appear clearly. The actual dechlorination reaction of 1,2-dichloroethane into ethylene would occur on silver. Used alone, this metal deactivates rapidly due to its covering by chlorine atoms. Thanks to its activation power of hydrogen by dissociative chemisorption, palladium present in the alloy supplies hydrogen atoms for the regeneration of the chlorinated silver surface into metallic silver. Let us mention that the palladium surface is partially covered by chlorine atoms as a consequence of their spillover from Ag to Pd. The presence of hydrogen adsorbed on Pd causes also the undesired ethylene hydrogenation leading to a loss of olefin selectivity.

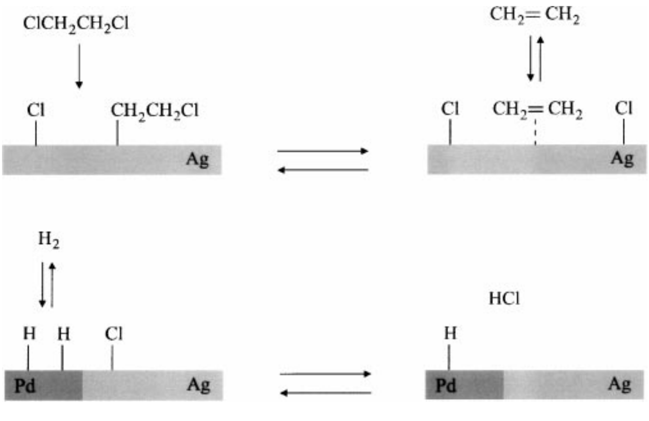

FIG. 3. Schematic representation of the mechanism suggested for 1,2-dichloroethane hydrodechlorination into ethylene on a Pd–Ag surface.

It is interesting to remark that such a reaction scheme of chlorination/hydrodechlorination of the silver surface shows a formal analogy with the oxidation/reduction mechanism of the catalytic surface proposed by Mars and van Krevelen for the oxidation of aromatic hydrocarbons (75). In that case, however, a reverse phenomenon occurs since the hydrocarbon is oxidized by reducing the catalytic surface which is reoxidized by gaseous oxygen:

Oxidation of aromatic hydrocarbons—Mars and van Krevelen mechanism (75)

(1) Aromatic hydrocarbon + oxidized catalyst → oxidation products + reduced catalyst

(2) Reduced catalyst + oxygen → oxidized catalyst

Selective hydrodechlorination of 1,2-dichloroethane into ethylene

(1) Chlorinated alkane + reduced catalyst → alkene + chlorinated catalyst

(2) Chlorinated catalyst + hydrogen → reduced catalyst

The next paper of this series will deal with the deactivation mechanisms and the regeneration of the Pd–Ag (33-67) hydrodechlorination catalyst.

APPENDIX

Roman Symbols

E_{a1}	Activation energy of rds1	J mmol^{-1}
E_{a2}	Activation energy of rds2	J mmol^{-1}
F_A	Molar flowrate of ethane at the reactor outlet	mmol s^{-1}
F_E	Molar flowrate of ethylene at the reactor outlet	mmol s^{-1}
F_{A0}	Molar flowrate of ethane at the reactor inlet	mmol s^{-1}
F_{E0}	Molar flowrate of ethylene at the reactor inlet	mmol s^{-1}
ΔH_i^0	Standard enthalpy change associated with elementary step i	J mmol^{-1}
K_i	Equilibrium constant of elementary step i	*

K_{0i}	Preexponential factor of K_i	$*$
$K_{\text{reaction 1}}$	Equilibrium constant of the reaction $ClCH_2–CH_2Cl + H_2 \leftrightarrow CH_2{=}CH_2 + 2HCl$	dimensionless
$K_{\text{reaction 2}}$	Equilibrium constant of the reaction $CH_2{=}CH_2 + H_2 \leftrightarrow CH_3–CH_3$	dimensionless
$K_{\text{reaction 3}}$	Equilibrium constant of the reaction $ClCH_2–CH_2Cl + 2H_2 \leftrightarrow CH_3–CH_3 + 2HCl$	dimensionless
k_1	Apparent kinetic constant associated with r_1	$*$
k_2	Apparent kinetic constant associated with r_2	$*$
k'_1	Intrinsic kinetic constant of rds1	$*$
k'_2	Intrinsic kinetic constant of rds2	$*$
k'_{01}	Preexponential factor of k'_1	$*$
k'_{02}	Preexponential factor of k'_2	$*$
p_{D}	Partial pressure of 1,2-dichloroethane	atm
p_{E}	Partial pressure of ethylene	atm
p_{H}	Partial pressure of hydrogen	atm
p_{HCl}	Partial pressure of hydrogen chloride	atm
R	Molar gas constant $= 8.3143 \times 10^{-3}$	$\text{J mmol}^{-1}\,\text{K}^{-1}$
r_{A}	Net ethane production rate	$\text{mmol kg}^{-1}\,\text{s}^{-1}$
r_{E}	Net ethylene production rate	$\text{mmol kg}^{-1}\,\text{s}^{-1}$
r_1	Rate of the irreversible reaction $ClCH_2–CH_2Cl + H_2 \rightarrow CH_2{=}CH_2 + 2HCl$	$\text{mmol kg}^{-1}\,\text{s}^{-1}$
r_2	Rate of the irreversible reaction $CH_2{=}CH_2 + H_2 \rightarrow CH_3–CH_3$	$\text{mmol kg}^{-1}\,\text{s}^{-1}$
r_3	Rate of the irreversible reaction $ClCH_2–CH_2Cl + 2H_2 \rightarrow CH_3–CH_3 + 2HCl$	$\text{mmol kg}^{-1}\,\text{s}^{-1}$
rds	Rate determining step in a sequence of elementary steps	
s	Active site	
T	Temperature	K
W	Catalyst mass inside the reactor	kg
w_1	Apparent reaction order in 1,2-dichloroethane associated with r_1	
w_2	Apparent reaction order in 1,2-dichloroethane associated with r_2	
x_1	Apparent reaction order in hydrogen associated with r_1	
x_2	Apparent reaction order in hydrogen associated with r_2	
y_1	Apparent reaction order in ethylene associated with r_1	
y_2	Apparent reaction order in ethylene associated with r_2	
z_1	Apparent reaction order in hydrogen chloride associated with r_1	
z_2	Apparent reaction order in hydrogen chloride associated with r_2	

Greek Symbols

σ	Stoichiometric number

Subscripts

i	Related to the ith step in a sequence of elementary steps
$*$	Dimensions of these variables depend on the system underconsideration.

ACKNOWLEDGMENTS

The authors are very grateful to Mr. C. Lebrun from the Solvay Company for his invaluable assistance during the kinetic data acquisition. B. Heinrichs thanks the Fonds pour la Formation à la Recherche dans l'Industrie et dans l'Agriculture, F.R.I.A., for a Ph.D. grant. The Ministère de la Région Wallonne, the Ministère de la Communauté Française de Belgique, and the Belgian F.N.R.S. are also gratefully acknowledged for financial support.

REFERENCES

1. Kalnes, T. N., and James, R. B., *Environ. Prog.* **7**, 185 (1988).
2. Bozzelli, J. W., Chen, Y.-M., and Chuang, S. S. C., *Chem. Eng. Commun.* **115**, 1 (1992).
3. Campbell, J. S., and Kemball, C., *Trans. Faraday Soc.* **57**, 809 (1961).
4. Anderson, J. R., and McConkey, B. H., *J. Catal.* **11**, 54 (1968).
5. Fung, S. C., and Sinfelt, J. H., *J. Catal.* **103**, 220 (1987).

6. Kovenklioglu, S., Cao, Z., Shah, D., Farrauto, R. J., and Balko, E. N., *AIChE J.* **38**, 1003 (1992).
7. Kim, S. Y., Choi, H. C., Yanga, O. B., Lee, K. H., Lee, J. S., and Kim, Y. G., *J. Chem. Soc., Chem. Commun.*, 2169 (1995).
8. Weiss, A. H., and Krieger, K. A., *J. Catal.* **6**, 167 (1966).
9. Gambhir, B. S., and Weiss, A. H., *J. Catal.* **26**, 82 (1972).
10. Kim, D. I., and Allen, D. T., *Ind. Eng. Chem. Res.* **36**, 3019 (1997).
11. LaPierre, R. B., Guczi, L., Kranich, W. L., and Weiss, A. H., *J. Catal.* **52**, 230 (1978).
12. Coq, B., Ferrat, G., and Figueras, F., *J. Catal.* **101**, 434 (1986).
13. Bodnariuk, P., Coq, B., Ferrat, G., and Figueras, F., *J. Catal.* **116**, 459 (1989).
14. Hagh, B. F., and Allen, D. T., *AIChE J.* **36**, 773 (1990).
15. Suzdorf, A. R., Morozov, S. V., Anshits, N. N., Tsiganova, S. I., and Anshits, A. G., *Catal. Lett.* **29**, 49 (1994).
16. Frimmel, J., and Zdrazil, M., *J. Catal.* **167**, 286 (1997).
17. Prins, R., *in* "Handbook of Heterogeneous Catalysis" (G. Ertl, H. Knözinger, and J. Weitkamp, Eds.), Vol. 4, p. 1908. Wiley–VCH, Weinheim, 1997.
18. LaPierre, R. B., Wu, D., Kranich, W. L., and Weiss, A. H., *J. Catal.* **52**, 59 (1978).
19. Fouilloux, P., Cordier, G., and Colleuille, Y., *Stud. Surf. Sci. Catal.* **11**, 369 (1982).
20. Ainbinder, Z., Manzer, L. E., and Nappa, M. J., *in* "Handbook of Heterogeneous Catalysis" (G. Ertl, H. Knözinger, and J. Weitkamp, Eds.), Vol. 4, p. 1677. Wiley–VCH, Weinheim, 1997.
21. Boyes, E. D., Coulson, D. R., Coulston, G. W., Diebold, M. P., Gai, P. L., Jones, G. A., Kellner, C. S., Lerou, J. J., Manzer, L. E., Mills, P. L., and Rao, V. N. M., *Proc. Am. Chem. Soc. Div. Petrol. Chem.* **38**, 847 (1993).
22. Kuznetsova, N. N., Lokteva, E. S., Lunin, V. V., and Yudina, S. L., *Kinet. Catal.* **36**, 121 (1995).
23. Karpinski, Z., Early, K., and d'Itri, J. L., *J. Catal.* **164**, 378 (1996).
24. Ribeiro, F. H., Gerken, C. A., Rupprechter, G., Somorjai, G. A., Kellner, C. S., Coulston, G. W., Manzer, L. E., and Abrams, L., *J. Catal.* **176**, 352 (1998).
25. Wiersma, A., van de Sandt, E. J. A. X., den Hollander, M. A., van Bekkum, H., Makkee, M., and Moulijn, J. A., *J. Catal.* **177**, 29 (1998).
26. Malinowski, A., Juszczyk, W., Bonarowska, M., Pielaszek, J., and Karpinski, Z., *J. Catal.* **177**, 153 (1998).
27. Öcal, M., Maciejewski, M., and Baiker, A., *Appl. Catal. B: Environ.* **21**, 279 (1999).
28. Kulkarni, P. P., Deshmukh, S. S., Kovalchuk, V. I., and d'Itri, J. L., *Catal. Lett.* **61**, 161 (1999).
29. Ito, L. N., Harley, A. D., Holbrook, M. T., Smith, D. D., Murchison, C. B., and Cisneros, M. D., International Patent Application WO 94/07827, 1994.
30. Ito, L. N., Harley, A. D., Holbrook, M. T., Smith, D. D., Murchison, C. B., and Cisneros, M. D., International Patent Application WO 94/07828, 1994.
31. Schoebrechts, J.-P., and Janssens, F., Demande de Brevet Internationale WO 96/16003, 1996.
32. Delhez, P., Heinrichs, B., Pirard, J.-P., and Schoebrechts, J.-P., U.S. Patent 6,072,096, 2000.
33. Ohnishi, R., Suzuki, I., and Ichikawa, M., *Chem. Lett.* **841** (1991).
34. Heinrichs, B., Delhez, P., Schoebrechts, J.-P., and Pirard, J.-P., *J. Catal.* **172**, 322 (1997).
35. Vadlamannati, L. S., Kovalchuk, V. I., and d'Itri, J. L., *Catal. Lett.* **58**, 173 (1999).
36. Heinrichs, B., Noville, F., Schoebrechts, J.-P., and Pirard, J.-P., *J. Catal.* **192**, 108 (2000), doi: 10.1006/jcat.2000.2816.
37. Froment, G. F., and Bischoff, K. B., "Chemical Reactor Analysis and Design." Wiley, New York, 1990.
38. Rylander, P. N., *in* "Catalysis: Science and Technology" (J. R. Anderson and M. Boudart, Eds.), Vol. 4, p. 1. Springer-Verlag, Berlin, 1983.
39. Heinrichs, B., "L'hydrodéchloration sélective du 1,2-dichloroéthane en éthylène sur des catalyseurs Pd–Ag/SiO$_2$," Ph.D. thesis, Université de Liège, Liège, 1999.
40. Heinrichs, B., Schoebrechts, J.-P., and Pirard, J.-P., *AIChE J.*, accepted for publication.
41. Himmelblau, D. M., "Process Analysis by Statistical Methods." Wiley, New York, 1970.
42. Press, W. H., Flannery, B. P., Teukolsky, S. A., and Vetterling, W. T., "Numerical Recipes in C—The Art of Scientific Computing," Cambridge Univ. Press, Cambridge, 1990.
43. Boudart, M., and Djéga-Mariadassou, G., "Kinetics of Heterogeneous Catalytic Reactions". Princeton Univ. Press, Princeton, 1984.
44. van Santen, R. A., and Niemantsverdriet, J. W., "Chemical Kinetics and Catalysis" Plenum, New York, 1995.
45. Boudart, M., "Kinetics of Chemical Processes." Prentice–Hall, Englewood Cliffs, NJ, 1968.
46. Kapteijn, F., and Moulijn, J. A., *in* "Handbook of Heterogeneous Catalysis" (G. Ertl, H. Knözinger, and J. Weitkamp, Eds.), Vol. 3, p. 1189. Wiley–VCH, Weinheim, 1997.
47. Yang, M. X., "Halogenated Hydrocarbons, Hydrogen Atoms and Metal Surfaces: Isolating Intermediates and Identifying Mechanisms in Catalytic Dehalogenation," Ph. D. thesis, Columbia University, New York, 1995.
48. Henderson, M. A., Mitchell, G. E., and White J. M., *Surf. Sci.* **184**, L325 (1987).
49. Anju, Y., Mochida, I., Yamamoto, H., Kato, A., and Seiyama, T., *Bull. Chem. Soc. Jpn.* **45**, 2319 (1972).
50. Wachs, I. E., and Kelemen, S. R., "Proceedings, 7th International Congress on Catalysis, Tokyo, 1980" (T. Seiyama and K. Tanabe, Eds.), Paper A48. Elsevier, Amsterdam, 1981.
51. Moss, R. L., and Thomas, D. H., *J. Catal.* **8**, 162 (1967).
52. Klugherz, P. D., and Harriott, P., *AIChE J.* **17**, 856 (1971).
53. Metcalf, P. L., and Harriott, P., *Ind. Eng. Chem. Process Des. Dev.* **11**, 478 (1972).
54. Barteau, M. A., and Madix, R. J., *Surf. Sci.* **103**, L171 (1981).
55. Schouten, E. P. S., Borman, P. C., and Westerterp, K. R., *Chem. Eng. Process.* **35**, 107 (1996).
56. van Santen, R. A., and Kuipers, H. P. C. E., *Adv. Catal.* **35**, 265 (1988).
57. Backx, C., de Groot, C. P. M., and Biloen, P., *Appl. Surf. Sci.* **6**, 256 (1980).
58. Kagawa, S., Iwamoto, M., Mori, H., and Seiyama, T., *J. Phys. Chem.* **85**, 434 (1981).
59. Huang, Y.-Y., *J. Catal.* **61**, 461 (1980).
60. Derouane, E. G., Pirard, J.-P., L'Homme, G. A., and Fabry-Volders, E., *in* "Catalysis: Heterogeneous and Homogeneous. Proceedings of the International Symposium on the Relations between Heterogeneous and Homogeneous Catalytic Phenomena, Brussels, Belgium, October 23–25, 1974,". Elsevier, Amsterdam, 1975.
61. Pirard, J.-P., and Kalitventzeff, B., *Ind. Eng. Chem. Fund.* **17**, 11 (1978).
62. van Santen, R. A., *in* "Handbook of Heterogeneous Catalysis" (G. Ertl, H. Knözinger, and J. Weitkamp, Eds.), Vol. 5, p. 2244. Wiley–VCH, Weinheim, 1997.
63. Backx, C., Moolhuysen, J., Geenen, P., and van Santen, R. A., *J. Catal.* **72**, 364 (1981).
64. Bergeret, G., and Gallezot, P., *in* "Handbook of Heterogeneous Catalysis" (G. Ertl, H. Knözinger, and J. Weitkamp, Eds.), Vol. 2, p. 439. Wiley–VCH, Weinheim, 1997.
65. Nieuwenhuys, B. E., *Stud. Surf. Sci. Catal.* **32**, 476 (1987).
66. Kok, G. A., Noordermeer, A., and Nieuwenhuys, B. E., *Surf. Sci.* **152/153**, 505 (1985).

67. Noordermeer, A., Kok, G. A., and Nieuwenhuys, B. E., *Surf. Sci.* **165**, 375 (1986).
68. Knor, Z., *in* "Catalysis: Science and Technology" (J. R. Anderson and M. Boudart, Eds.), Vol. 3, p. 231. Springer-Verlag, Berlin, 1982.
69. Pirard, J.-P., "Approche Multidisciplinaire d'un Problème de Catalyse Hétérogéne—L'Hydrogénation de l'Ethylène par le Cuivre Déposé sur l'Oxyde de Magnésium," Ph.D. thesis, Université de Liège, Liège, 1974.
70. Pajonk, G. M., *in* "Handbook of Heterogeneous Catalysis" (G. Ertl, H. Knözinger, and J. Weitkamp, Eds.), Vol. 3, p. 1064. Wiley–VCH, Weinheim, 1997.
71. Dumesic, J. A., Rudd, D. F., Aparicio, L. M., Rekoske, J. E., and Treviño, A. A.,. "The Microkinetics of Heterogeneous Catalysis," Am. Chem. Soc., Washington, DC, 1993.
72. Bond, G. C., "Catalysis by Metals." Academic Press, New York, 1962.
73. Sachtler, W. M. H., *in* "Handbook of Heterogeneous Catalysis" (G. Ertl, H. Knözinger, and J. Weitkamp, Eds.), Vol. 3, p. 1077. Wiley–VCH, Weinheim, 1997.
74. Allison, E. G., and Bond, G. C., *Catal. Rev.* **7**, 233 (1972).
75. Mars, P., and van Krevelen, D. W., *Chem. Eng. Sci. Special Suppl.* **3**, 41 (1954).